PHYSICAL REVIEW D **81,** 075006 (2010)

A strong sector at the LHC: Top partners in same-sign dileptons

Jan Mrazek* and Andrea Wulzer†

Institut de Théorie des Phénomènes Physiques, École Polytechnique Fédérale de Lausanne, CH-1015, Lausanne, Switzerland, USA

(Received 22 December 2009; published 9 April 2010)

Heavy partners of the top quark are a common prediction of many models in which a new strongly-coupled sector is responsible for the breaking of the electroweak symmetry. In this paper, we investigate their experimental signature at the LHC, focusing on the particularly clean channel of same-sign dileptons. We show that, thanks to a strong interaction with the top quark which allows them to be singly produced at a sizable rate, the top partners will be discovered at the LHC if their mass is below 1.5 TeV, higher masses being possible in particularly favorable (but plausible) situations. Since the partners are expected to be lighter in both the Higgsless and composite-Higgs scenarios, then one of same-sign dileptons is found to be a very promising channel in which these models could be tested. We also discuss several experimental signatures which would allow, after the discovery of the excess, to attribute it uniquely to the top partners production and to measure the relevant physical parameters, i.e. the top partners' masses and couplings. We believe that our results constitute a valid starting point for a more detailed experimental study.

DOI: 10.1103/PhysRevD.81.075006 PACS numbers: 12.60.Cn

I. INTRODUCTION

Models in which a new strongly-coupled sector is responsible for the electroweak symmetry breaking (EWSB), solving the hierarchy problem, have received renewed attention in the last few years. Progress came from warped compactifications [1] which allowed the reformulation of old scenarios such as technicolor [2] and composite-Higgs [3] in terms of calculable five-dimensional (5D) effective theories leading, respectively, to the Higgsless [4–6] and to the minimal composite-Higgs models [7,8].

It is far from established that any of these 5D models is exactly dual to some four-dimensional (4D) strong dynamics, but it is known that striking similarities exist. Compatible with our qualitative understanding of strongly-coupled dynamics, any 5D model result can be consistently interpreted in 4D language. For phenomenological purposes, however, the 5D models could be considered per sé and their validity as effective field theories might well extend above the maximum energy reach of the LHC. Moreover, their UV completion could come from string theory rather than from a strong sector. If this is the case, the strongly-coupled language would just be a useful tool to give an alternative (and sometimes simpler) interpretation to the 5D-theory results.

The 5D models not only provided a calculable realization of previous scenarios, they also suggested new model-building solutions. It is the case of the "partial compositeness" idea (originally proposed in [9]) which is automatically implemented in the 5D construction [10] and actually constitutes its key feature in terms of which much of the 5D physics can be captured by simple 4D models [11]. In partial compositeness, the standard model (SM) fermions f (similarly to the SM vector bosons which mix with the currents) couple to the strong sector, and therefore acquire their mass after EWSB, by mixing linearly with some strong-sector operator $\mathcal{O}$, i.e. through terms like $f\mathcal{O}$ in the UV Lagrangian. In the IR, where a mass gap is generated, a composite fermion with the quantum numbers of $\mathcal{O}$ exists and the UV term is converted into a mixing of the SM fermion with this composite state. After EWSB, the mass eigenstates are a light SM fermion and its heavy partner, with mass of the TeV order. Since small masses require small mixings, the light SM families are mostly elementary and very weakly coupled to the strong sector. This realizes the so-called Randall-Sundrum–Glashow-Iliopoulos-Maiani mechanism of flavor protection [12] which almost, but not completely [13], solves the long-standing flavor problem of previous strong-sector EWSB models. Among the partners, the one of the top quark is special and is the subject of our study. To acquire its high mass, indeed, the top quark must have a sizable composite component and therefore sizable interactions with the strong sector and, in particular, with its partner. These interactions could make deviations from the SM of the top interactions detectable [14] and they play a major role in our study of the top partners production at the LHC.

The existence of top partners is a generic and robust prediction of the 5D models and, more generally, of 5D-inspired partial compositeness scenarios [11]. Another signature is massive vector resonances in the adjoint of the color group; the latter are expected to be present if the strong sector carries color as it must in partial compositeness in order for the strong-sector operators $\mathcal{O}$ to mix with the quarks. These resonances are the partners of the gluon in the language of [11] and arise as Kaluza-Klein gluons in the 5D models, their production and decay to tops should

*jan.mrazek@epfl.ch
†andrea.wulzer@epfl.ch

be observable at the LHC if their mass is below about 4 TeV [15]. The most direct and robust signature of strong-sector EWSB (independently on whether it realizes partial fermion compositeness or not) would however be the detection of color-singlet vectors with electroweak (EW) quantum numbers, essentially analog to the QCD ρ mesons. The latter are the partners (or the Kaluza-Klein, in the 5D language) of the EW gauge bosons and play a crucial role in the WW scattering unitarization even in the case of a composite Higgs at high enough energies. These states will be visible at the LHC only if they are lighter than about 2 or 3 TeV [16]. The EW partners, however, directly contribute to the S parameter at tree level, and in the absence of cancellations their mass should be higher than a few ($\gtrsim 3$) TeV in order for the model to be compatible with precision EW measurements [8,17]. In the Higgsless model, the EW partners are forced to be light, and therefore possibly visible at the LHC, since they are the solely responsible for WW unitarization. This requires a fine-tuning in S which renders the model less appealing.[1] In the composite-Higgs case, on the contrary, the EW partners masses (or, which is the same, the strong-sector compositeness scale Λ) can be above 3 TeV without violating perturbative unitarity due to the presence of a Higgs particle which can postpone unitarity violation to higher energies. This is achieved by a fine-tuning in v/f, where $v = 246$ GeV is the Higgs vacuum expectation value (VEV) and f is the decay constant of the Higgs, which arises as a Goldstone boson in these models. Making f large, the EW partners become heavy and no extra fine-tuning is needed in S. The EW partners, however, will be invisible at the LHC and it becomes difficult, more in general, to probe the strongly-coupled nature of the Higgs sector [18].

In this paper, we study the possibility of observing the top partners in the extremely clean channel of two same-sign hard and separated leptons, large total transverse energy H_T, and some missing energy $\not{E}_T$. We will show that discovery is possible, if the coupling to tops is large as expected, up to 1.5 TeV top partner mass, but it becomes difficult if they are heavier. The channel we study is therefore relevant for the Higgsless case, in which the strong scale Λ is low and it is natural to have top partners below 1.5 TeV, while it might appear marginal in models with Λ of about 3 TeV. This is not the case, however, in the compelling composite-Higgs scenario where, as discussed in detail in [8], the top partners are always parametrically lighter than Λ and lie in the [0.5, 1.5] TeV mass range. This happens in all of the allowed parameter space and independently on details of the model such as the 5D representations in which the SM fermions are embedded. An heuristic explanation of this is that the Higgs mass term, which is finite and calculable in these models, is the result of a cancellation between the low-energy SM-like contribution and the high-energy contribution of the new states. The bigger SM contribution comes from the top loops and is canceled by the top partners loops (which play in this context essentially the same role as the stop loops in supersymmetry) while the SM gauge fields loops are canceled by the EW partners contribution. But the Higgs is light (below 190 GeV) in these models, which is also helpful with EWPT, and requiring an upper bound on m_h enforces an upper bound on the mass of the partners, which have to be light enough for the SM divergence cancellation to begin at small enough energies. The most stringent bound is on the top partners, since their role is to cancel the larger SM contribution, while the EW partners are allowed to be heavier. Along the lines above, the bound of 1.5 TeV on the top partners mass can be derived, and a correlation of the top partners mass with the Higgs mass is established; we refer the reader to [8] for a complete discussion. Summarizing, top partners in the [0.5, 1.5] TeV range are likely to be the best experimental signature of the composite-Higgs scenario, all other new states being expected sensibly heavier.

The production of heavy colored fermions at the LHC has been extensively studied [19,20], but the analysis which is more closely related to ours is the one of Ref. [21], which also considered top partners in same-sign dileptons. While Ref. [21] focused on pair production, we also consider the single production mediated by the previously discussed interaction with the top quark. Since the latter is the distinctive feature of the top partner, the inclusion of this production channel will help to distinguish it from a generic colored heavy fermion and will permit, as we will discuss, a simple measurement of the coupling. Moreover, the single production greatly enhances the cross section for high masses and makes discovery possible in the entire range of interest. At the technical level, our event-selection strategy differs from the one of [21]. We indeed find an H_T cut to be extremely efficient in reducing the background. Our selection makes only use of this variable, of the leptons momenta, and of some $\not{E}_T$. We include in our analysis the experimental effect of charge misidentification which is potentially important for same-sign dileptons due to the very large opposite-sign SM background. We make the conservative assumption of 1% flat charge misidentification probability (typical lepton $p_T 100 < p_T < 500$ GeV) and with this assumption one main background is an opposite-sign process. Our results could therefore improve if charge misidentification is closer to 10^{-3} as expected. We also discuss how, after the discovery of the excess, the underlying exotic particle content could be identified and the masses and couplings of the top partners measured, we believe that our result are a

[1]It is actually the request of an enhanced calculability (i.e. of a large number of colors N_c) which, combined with WW unitarization, implies low EW partners mass. In a QCD-like case ($N_c = 3$), the partners should be as heavy as 2.5 TeV and a moderate tuning would be sufficient.

valid starting point for a more detailed experimental analysis.

II. THE MODEL

We describe the top partners using the language of partial compositeness, that provides a simple parametrization of 5D strong-sector EWSB models [11]. We therefore introduce heavy vectorlike colored fermions Q and $\tilde{T}$ which are the partners of, respectively, the standard $q_L = (t_L, b_L)$ doublet and the t_R singlet; we ignore light families and the b_R partners since they will not play a role in what follows. The strong sector, which generates the partners, is assumed to respect a global $G_s = SU(2)_L \times SU(2)_R \times U(1)_X$ symmetry, where the SM $SU(2)_L$ is embedded in the first factor while for the hypercharge, we have $Y = T_3^R + X$. The first $SU(2)_L \times SU(2)_R \simeq SO(4)$ factor will be spontaneously broken down to the custodial $SO(3)_c$, either by the strong sector itself as in the Higgsless scenario or by the Higgs VEV in the composite Higgs, making in both cases purely strong-sector contributions to the T parameter vanish. The partners therefore live in representations of G_s, and since their role is to give a mass to the top quark, they must be chosen such that a G_s-invariant "proto-Yukawa" term for them exists and at the same time they can mix with the SM fermions without breaking the SM group. This last requirement actually forces the strong sector to carry color as an additional global symmetry; the group is $SU(3)_c \times G_s$ and the partners are color triplets.

Both cases in which the strong sector delivers a Higgs field or not can be treated simultaneously if we write

$$H = \begin{bmatrix} h_d^\dagger & h_u \\ -h_u^\dagger & h_d \end{bmatrix} = \frac{v}{\sqrt{2}} U \simeq \begin{bmatrix} \frac{1}{\sqrt{2}}(v - i\varphi_0) & \varphi_+ \\ -\varphi_- & \frac{1}{\sqrt{2}}(v + i\varphi_0) \end{bmatrix}, \quad (1)$$

where H is the Higgs field, in the $(\mathbf{2}, \mathbf{2})_\mathbf{0}$ of G_s, U is the Goldstone bosons' unitary matrix parametrized by the neutral (φ_0) and charged ($\varphi_- = \varphi_+{}^\dagger$) Goldstone fields, and the last approximate equality is obtained by expanding U at the first order in the Goldstones. In the case of a composite Higgs, v should be a dynamical degree of freedom whose fluctuations describe the physical Higgs boson, but since we are not interested in interactions of the partners with the physical Higgs, we have set it to its VEV $v = 246$ GeV. We will write the proto-Yukawa interactions in terms of H, but after making use of Eq. (1), we will obtain the same Lagrangian we would have written in the Higgsless case where only the Goldstones in U (and not the entire H) are present. What we denote as the proto-Yukawa term is actually, in the Higgsless case, a non-$SO(4)$ invariant mass term properly "dressed" with Goldstones in order for the $SO(4)$ symmetry to be restored.

The concrete model we consider is the same as in [21], which provides a parametrization of the composite-Higgs model of [8] and of the Higgsless model of [5]. The top partner representations and the associated proto-Yukawa term are

$$Q = (\mathbf{2}, \mathbf{2})_{2/3} = \begin{bmatrix} T & T_{5/3} \\ B & T_{2/3} \end{bmatrix}, \qquad \tilde{T} = (\mathbf{1}, \mathbf{1})_{2/3}, \qquad \mathcal{L}_Y = Y_t^* \,\mathrm{Tr}[\bar{Q} H]\tilde{T} + \mathrm{H.c.}, \quad (2)$$

where the (T, B) doublet has the same SM quantum numbers as $q_L = (t_L, b_L)$, and $\tilde{T}$ has the ones of t_R. The Q and $\tilde{T}$ multiplets have masses $M_{Q,\tilde{T}}$ of the order (though a bit smaller in the composite-Higgs case, as we have discussed) of the compositeness scale $\Lambda \sim$ TeV, and also mix with strength $\Delta_{Q,\tilde{T}}$ to q_L and t_R. Diagonalizing the mixings, one gets a mass term for the top. From Eq. (2), we find

$$y_t = \frac{\sqrt{2} m_t}{v} = Y_t^* \sin\varphi_q \sin\varphi_t, \quad (3)$$

where $\varphi_{q,t}$ are the q_L, t_R mixing angles.

The equation above immediately tells us that the proto-Yukawa coupling Y_t^* cannot be very small; it has at least to exceed $y_t \simeq 1$. It will actually be bigger in concrete models, because of the following. If Y_t^* is generated by strong dynamics (or by an extra-dimensional model), it can be estimated as

$$Y_t^* = \frac{4\pi}{\sqrt{N}},$$

where N is the number of colors of the strong sector. In the 5D language, $1/\sqrt{N}$ corresponds to the expansion parameter and indeed making N big makes our IR description of the strong sector more weakly coupled. A strong bound on the number of colors N comes from the S parameter which grows linearly with N as a result of the fact that the vector resonances mass m_ρ decreases (at fixed $4\pi f \sim m_\rho \sqrt{N}$) as $1/\sqrt{N}$. This requires $N \lesssim 10$ [8] which in turn implies $Y_t^* \gtrsim 4$. As an upper bound on Y_t^*, which could still ensure calculability in the 5D model, we could take for instance the g_ρ coupling of the ρ meson of QCD which corresponds to $N = 3$ and is around 6.

The Lagrangian in Eq. (2) also delivers top partner interactions with two SM particles, which will mediate top partner decay and single production. These are

$$\begin{aligned} \mathcal{L}_Y = & -Y_t^* \sin\varphi_t \cos\varphi_q \varphi_+ \bar{t}_R B + Y_t^* \sin\varphi_t \varphi_- \bar{t}_R T_{5/3} \\ & + i Y_t^* \sin\varphi_t \cos\varphi_q \frac{\varphi_0}{\sqrt{2}} \bar{t}_R T - i Y_t^* \sin\varphi_t \frac{\varphi_0}{\sqrt{2}} \bar{t}_R T_{2/3} \\ & - Y_t^* \sin\varphi_q \cos\varphi_t \left[\varphi_- \bar{b}_L + i \frac{\varphi_0}{\sqrt{2}} \bar{t}_L \right] \tilde{T} + \mathrm{H.c.}, \end{aligned} \quad (4)$$

and correspond, when going to the unitary gauge and making use of the Equivalence Theorem, to vertices with the longitudinal EW bosons. From the Lagrangian above, it is easy to see that only the B and the $T_{5/3}$ partners will be

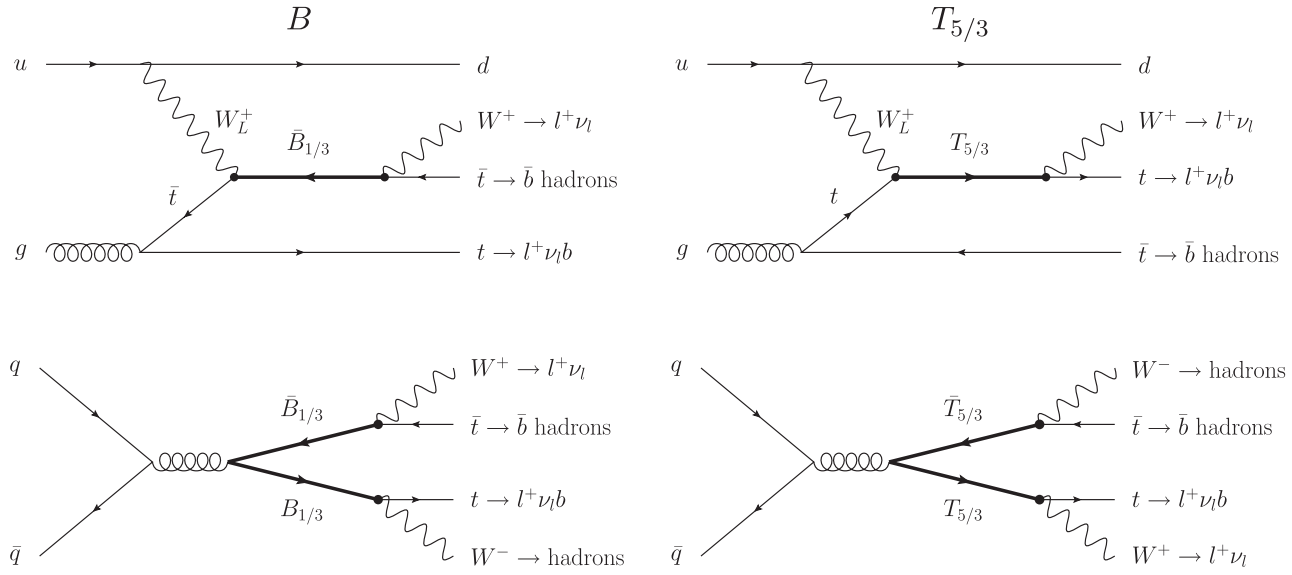

FIG. 1. Typical single and pair production diagrams for $T_{5/3}$ and B for signals with two positively charged leptons. We notice that for $T_{5/3}$, the lepton always comes from its decay, while for B they originate in two different legs.

visible in the final state we want to study, which contains two hard and separated same-sign leptons; the pair and single production diagrams are shown in Fig. 1.

The couplings $\lambda_B = Y_t^* \sin\varphi_t \cos\varphi_q = y_t/\tan\varphi_q$ and $\lambda_T = Y_t^* \sin\varphi_t = y_t/\sin\varphi_q$ are potentially large since Y_t^* is large, as we have discussed, and for sure $\lambda_T \geq y_t \simeq 1$. But they will actually be bigger in realistic models where the amount of compositeness of q_L, $\sin\varphi_q$, cannot be too large. The b_L couplings have indeed been measured with high precision and showed no deviations from the SM. Large b_L compositeness would have already been discovered, for instance in deviations of the $Zb_L\bar{b}_L$ coupling from the SM prediction. Generically, corrections $\delta g_L/g_L \sim \sin\varphi_q^2 (v/f)^2$ [11] are expected which would imply (for moderate tuning $v/f \ll 1$) an upper bound on $\sin\varphi_q$. It is however possible to eliminate such contributions by imposing, as in the model of [8] (see also [22]), a "custodial symmetry for $Zb_L\bar{b}_L$" [23] which makes the correction reduce to $\delta g_L/g_L \sim \sin\varphi_q{}^2 (m_Z/\Lambda)^2$. Still, having not too large of a b_L compositeness is favored, and further bounds are expected to come from flavor constraints in the B-meson sector. To be more quantitative, we can assume that $\sin\varphi_q < \sin\varphi_t$, i.e. that q_L is less composite than the t_R. This implies $\sin\varphi_q < \sqrt{(y_t/Y_t^*)}$ and therefore $\lambda_T > \sqrt{(y_t Y_t^*)} \gtrsim 2$ and $\lambda_B > \sqrt{(y_t Y_t^* - y_t^2)} \gtrsim \sqrt{3}$. We will therefore consider $\lambda_{T,B}$ couplings which exceed 2 and use the reference values of 2, 3, 4; smaller values for both couplings are not possible under the mild assumption $\sin\varphi_q < \sin\varphi_t$.

Our analysis, though performed in the specific model we have described, has a wide range of applicability. The existence of the B partner is, first of all, a very general feature of the partial compositeness scenario given that one partner with the SM quantum numbers of the b_L must exist. Also, it interacts with the t_R as in Eq. (4) due to the $SU(2)_L$ invariance of the proto-Yukawa term. The $T_{5/3}$ could, on the contrary, not exist; this would be the case if for instance we had chosen representations $Q = (\mathbf{2}, \mathbf{1})_{1/6}$ and $\tilde{T} = (\mathbf{1}, \mathbf{2})_{1/6}$ for the partners (which is however strongly disfavored by combined bounds from $\delta g_b/g_b$ and T), or in the model of [11]. To account for these situations, we will also consider the possibility that only the B partner is present.[2] The existence of the $T_{5/3}$ is a consequence of the $Zb_L\bar{b}_L$-custodial symmetry, which requires that the B partner has equal T_L^3 and T_R^3 quantum numbers. This, plus the $SO(4)$ invariance of the proto-Yukawa, implies that the $T_{5/3}$ must exist and couple as in Eq. (4). Our analysis, as we have remarked, can also apply to Higgsless scenarios in both cases in which the custodian $T_{5/3}$ is present or not. The results could change quantitatively in other specific models, because for instance other partners can be present and contribute to the same-sign dilepton signal, or other channels could open for the decay of the partners making the branching ratio to top decrease, which is one in our model. This cannot however qualitatively invalidate our conclusions on the discovery, which are robust if the partners are not too heavy and their couplings, which determine the single production cross section, are not too small.

[2]In this case, our analysis perfectly applies to the model proposed in [11], where the t_R is entirely composite, $\sin\varphi_t = 1$, and the coupling is large.

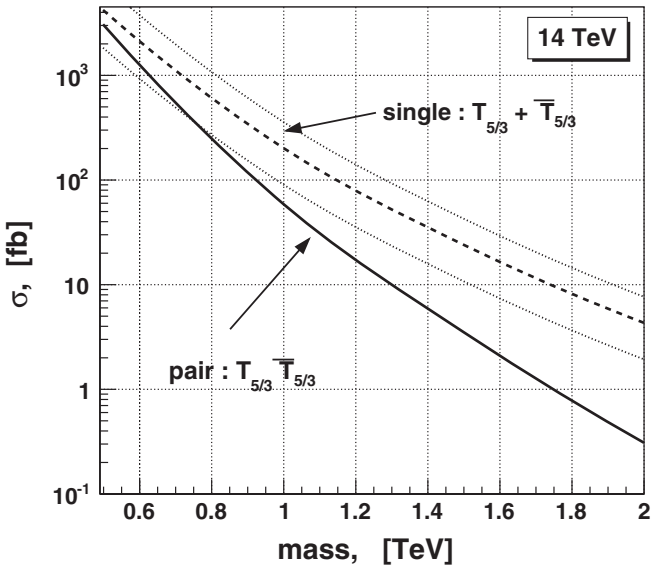

FIG. 2. Cross sections, summed over charge, for pair (plain) and single (dashed) production of $T_{5/3}$ (or B) as a function of its mass. The dotted lines show the effect for the single production of varying $2 < \lambda_{T,B} < 4$.

III. DISCOVERY ANALYSIS

The cross sections of single and pair top partners production at the LHC are shown in Fig. 2. After production, the partners decay to top quark and W as depicted in Fig. 1 with unit branching ratio, but reaching the dilepton final state will cost us an extra factor of $\approx \frac{2}{9} \cdot \frac{2}{9} \cdot \frac{6}{9} \approx 0.03$ (id. $\cdot \frac{6}{9} \approx 0.02$) for single (pair) production. Compared with pair, the single production cross section is always sizable in the mass range we are interested in and, since it decreases slower with the top partner mass, rapidly becomes dominant. This is somewhat surprising, since the single production diagram contains one weak interaction vertex and is also suppressed, in comparison with pair production, by the three-body phase space. Very similar situations, however, are encountered in the case of a fourth heavy family production, studied in [24], and in the phenomenology of little Higgs models [20].

The main reason for the single production enhancement (or which is the same, for the pair production suppression) is explained by Fig. 3, where the single and pair production partonic cross sections are shown as a function of the partonic center-of-mass energy $\sqrt{\hat{s}} = x_1 x_2 \sqrt{S}$ (where $\sqrt{S} = 14$ TeV and $x_{1,2}$ are the parton momenta fractions) for, respectively, qg and gg initial states and the 1 TeV top partner mass. Even though the latter is bigger by a factor ≈ 10 in the first 500 GeV $\sqrt{\hat{s}}$ slice, it starts at higher $\sqrt{\hat{s}}$ ($\sqrt{\hat{s}} > 2M$) while the threshold is lower ($\sqrt{\hat{s}} > M + m_t$) in the single production case. The partonic cross sections will have to be convoluted with the corresponding differential partonic luminosities which are defined as

$$\frac{d\mathcal{L}_{i,j}}{d\hat{s}} = \frac{1}{S} \int_{\hat{s}/S}^{1} \frac{dx}{x} F_i(x) F_j(\hat{s}/(Sx)),$$

and shown in Fig. 3, computed using the Martin-Stirling-Thorne-Watt parton distribution functions grids [25] with $Q = 2$ TeV. It is immediate to see that, since the differential luminosities decrease exponentially, the integrated one in the $[M + m_t, 2M]$ range is much larger than the one from $2M$ and $\sqrt{S}$. The pair production total cross section, which only receives contributions from the second $\sqrt{\hat{s}}$ interval ($\sqrt{\hat{s}} \in [2M, \sqrt{S}]$), is suppressed with respect to single by a large factor. For the 1 TeV case, the suppression factor is approximately given by $\mathcal{L}_{i,j}(2M)/\mathcal{L}_{i,j}(M + m_t) \sim 1/20$, which is enough to compensate for the different partonic cross sections of the two processes. Also, the

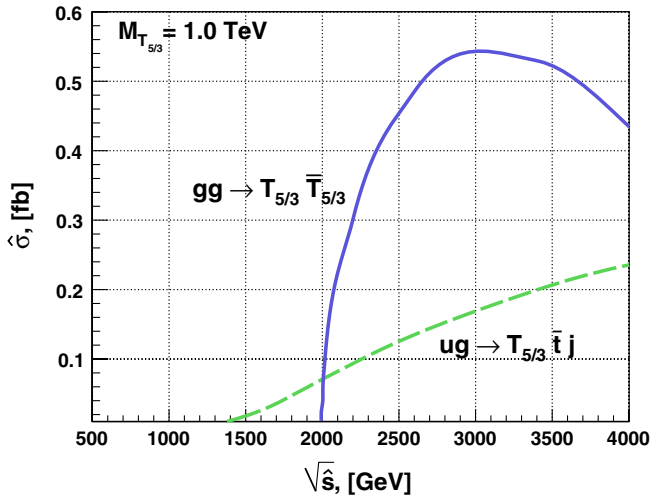

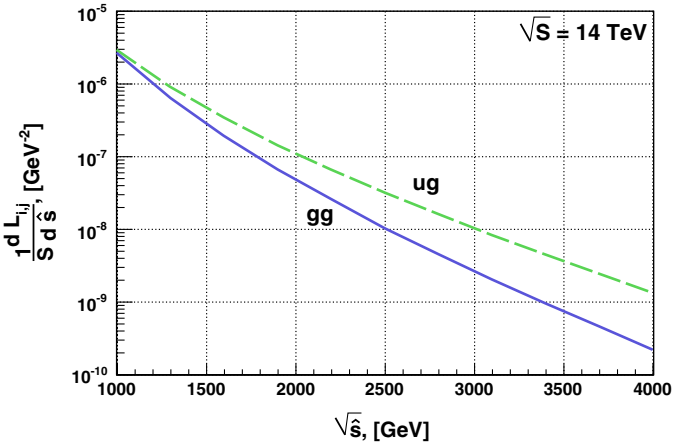

FIG. 3 (color online). On the left, the partonic cross section for two typical contributions to single ($ug \to T_{5/3}\bar{t}$; $\lambda = 3$) and pair ($gg \to T_{5/3}\bar{T}_{5/3}$) production. To find the total cross sections, these have to be convoluted with the corresponding partonic luminosities which are shown on the right for ug and gg as function of $\sqrt{\hat{s}}$.

suppression factor decreases for higher masses, and this explains why the single production process is comparatively more important for higher masses, as Fig. 2 shows.

Notice that, as discussed in [24], the single production process can be considered as a W-gluon fusion because the intermediate W tends (in order to maximize its propagator) to have low virtuality, of order $-m_w^2$, while still carrying enough energy to produce the heavy partner. This makes the final state partonic line from which the W is emitted to be very forward, leading to a forward jet similar to the ones of W-boson fusion Higgs production [26]. For $p_T \lesssim m_w$, and an energy around the TeV, the forward jet will have rapidity $\eta \gtrsim 3$; the presence of this forward jets constitutes an important feature of our signal which we will discuss in more detail in the following.

A. Signal and background

The one of same-sign dileptons is a very clean channel in which the single and pair production of the top partner can be observed. The decay chains leading to positively charged leptons for both the B and $T_{5/3}$ production are shown in Fig. 1; the case of negative charge final leptons can be easily worked out. Notice that while the pair production process contributes the same to both charges, single production leads to a charge asymmetry. The hard initiating parton, which has to provide most of the energy for producing the partner, is indeed preferentially a valence quark and specifically an up in the (l^+, l^+) case and a down for (l^-, l^-). We therefore have a factor of roughly two between the single production contribution to the positive and negative charge signal. This leads to a sizable charge asymmetry that could be exploited to measure the single production cross section and eventually the top partner coupling, as we will discuss.

Not to enter in subtleties of τ reconstruction, we only consider electrons and muons and also, in order to neglect leptons from heavy flavors and jet/lepton misidentification, we require leptons to be separated from hadronic activity with a separation cut $\Delta R(LJ) > 0.4$. Also, our leptons should be hard enough ($p_T > 10$ GeV) and of course inside the detector ($\eta < 2.5$). Since there are also neutrinos, our signal is in conclusion $pp \to l^\pm l^\pm + \not{E}_T + n$ jets with hard and separated leptons. Notice that the separation cut, in the case of very high mass, starts becoming costly for $T_{5/3}$ since the leptons come from boosted tops and tend to be close to the b jet. This does not represent a problem for $M_T \lesssim 1.5$ TeV, but above it is a serious limitation. But in this case, independent of this effect, discovery in the dilepton channel will become hard due to the decrease of the cross section worsened by the small leptonic W branching ratio. In order to go further, hadronic W final states should be included and advanced techniques of boosted top reconstruction (see for example [15]) will be needed.

The background, because of our isolation and hardness cuts, comes from the production of SM heavy particles subsequently decaying to leptons. Processes in which exactly two same-sign leptons are produced are $W^\pm W^\pm$, $t\bar{t}W^\pm$, $W^\pm W^\pm W^\mp$, and $t\bar{t}W^+W^-$ where the latter two are competitive with the former if the SM Higgs is heavy enough to give a resonant contribution to the W^+W^- pair production. To maximize this possibility, we have assumed this to be the case and have chosen the Higgs mass to be $m_H = 180$ GeV. Notice that we label the background processes only in terms of their heavy SM particles content, but we will take into account additional hadronic activity they might also include. Strictly speaking, the suffix "$+n$ jets" should be attached to all of our background process names. There are also processes in which three leptons are produced but one is lost, either outside the detector ($\eta > 2.5$) or below threshold, which we set at 5 GeV. The only such relevant process is $W^\pm Z$ which, despite the geometrical suppression factor for losing a lepton, is competitive with $W^\pm W^\pm$ since the latter final state starts being produced, necessarily in association with at least two partons, to a higher α_S order. The $W^\pm W^\pm Z$ process is on the contrary subdominant compared with $W^\pm W^\pm W^\mp$ and can be neglected.

All of the backgrounds listed up to now will be referred to as *true background*, while a second very important source of background, originating because of charge misidentification, will be denoted as *sign background*. The latter are $t\bar{t}$, Z^*/γ^* and W^+W^- whose cross sections are clearly much larger than those of the true backgrounds we have listed. Their real impact on our analysis depends on the charge misidentification probability of the detector which is hard to estimate, because it strongly depends on the p_T and rapidity of the leptons, as well as on the detector and the lepton species (muons are typically better identified that electrons, for instance). On top of this, it has been only poorly covered in the literature in the case of lepton momenta $p_T \sim 100$–500 GeV, which is the region we are interested in. We will therefore use a flat charge misidentification probability of 1% believing this to be a conservative assumption, which rates closer to 10^{-3} (or even less for muons), as expected [27].

1. Simulation

We generated signal and background events using MADGRAPH/MADEVENT [28], with higher order emissions of extra parton taken into account.[3] Showering was performed with PYTHIA [29], where hadronization, which should not play any role in our analysis, was turned off. For each process, we generated matrix element events with different final state partons content and, after showering, different matrix elements were combined by the Michelangelo Mangano (MLM) matching prescription with k_T jet algorithm [30–32]. Finally, jets were reconstructed using the Paige's cone jet algorithm implemented

[3]We are indebted with R. Contino for providing us with the MADGRAPH model for the top partners.

in GETJET [33], with parameters $\Delta R = 0.7$, $E_{\rm min} = 20$ GeV. The resulting cross sections are shown in Table I where for each process the different matrix elements combined by MLM matching are also reported. The cross sections of Table I are for hard and separated leptons inside the detector, as previously specified, but a cut $M(LL) > 120$ GeV was also implemented. The latter is needed to forbid real Z production to contribute to the Drell-Yan Z^*/γ^* background. Also, the suppression factor of 10^{-2} for charge misidentification is already taken into account.

The detailed simulation described above, including MLM matching, was performed in order to obtain as realistic samples of events as possible, on which the more detailed analysis of the top partners, which we will discuss in Sec. IV, can be reliably performed. The discovery results presented in this section, however, do not rely on this detailed simulation. For event selection, we will indeed not use observables, such as for instance the number of jets, which require a detailed knowledge of the hadronic structure of the event. We have checked explicitly that the results of the present section can be reproduced by pure matrix element simulations with additional hard QCD contributions. This makes our analysis more robust.

In addition to the lepton charge misidentification, we have included the detector effect of fake $\not{E}_T$ [27]. A cut on $\not{E}_T$ is indeed very useful to get rid of the Z^*/γ^* background, but fake $\not{E}_T$ is crucial for a realistic estimate of the efficiency of this cut. Both for ATLAS and CMS, the error on the each component of the missing p_T can be estimated by a Gaussian distribution with a width given by the activity inside the detector:

$$\sigma = \kappa \sqrt{\sum_{\rm jet,lep} |p_T|}, \tag{5}$$

where for ATLAS $\kappa = 0.46$, while $\kappa = 0.97$ for CMS [27]. We use $\kappa = 1.0$ and, at the stage of the analysis of the simulated events, add a random δp_T fluctuation to the missing p_T.

TABLE I. Cross sections for the various processes after a minimal set of cuts, $p_T(L) > 10$ GeV, $M(LL) > 120$ GeV; a charge misidentification probability of 10^{-2} is taken into account. The single production cross section is for $\lambda_{T,B} = 3$, by varying λ it scales as λ^2.

	$\sigma(l^+l^+)$, [fb]	$\sigma(l^-l^-)$, [fb]
$T_{5/3} + B$, $M = 0.5$ TeV	84.6	45.2
$T_{5/3} + B$, $M = 1.0$ TeV	5.00	2.49
$T_{5/3} + B$, $M = 1.5$ TeV	0.596	0.272
$T_{5/3} + B$, $M = 2.0$ TeV	0.116	0.041
$T_{5/3}T_{5/3} + BB$, $M = 0.5$ TeV	67.0	67.0
$T_{5/3}T_{5/3} + BB$, $M = 1.0$ TeV	1.47	1.47
$T_{5/3}T_{5/3} + BB$, $M = 1.5$ TeV	0.076	0.076
$T_{5/3}T_{5/3} + BB$, $M = 2.0$ TeV	0.0053	0.0053
$t\bar{t} + 0, 1, 2$ j	56.7	56.7
$Z^*/\gamma* + 0, 1, 2, 3$ j	168.0	168.0
$W + W - + 0, 1, 2$ j	5.83	5.83
$t\bar{t}W^{\pm} + 0, 1, 2$ j	2.25	1.52
$W^{\pm}Z + 0, 1, 2$ j	7.66	4.44
$W^{\pm}W^{\pm} + 2, 3$ j	2.87	1.60
$W^{\pm}W^{\pm}W^{\mp} + 0, 1, 2$ j	1.97	1.28
$t\bar{t}W^{\pm}W^{\mp} + 0, 1$ j	0.595	0.595

B. Event selection

The dominating background, as Table I shows, is Z^*/γ^*, but this will become substantially irrelevant when a cut on $\not{E}_T$ will be applied. Second comes $t\bar{t}$ which will be more difficult to get rid of. The choice of the observables and their optimization focuses on the single production, which is the relevant production mechanism in the range of high masses where discovery becomes less easy. Our search strategy, however, turns out to be efficient for pair production as well. The first observables we focus on are the p_T of the hardest and second hardest leptons, L_1 and L_2, whose distributions are shown Fig. 4. Notice that the leptons are typically softer for B than for $T_{5/3}$, but this had to be expected, since in the second case both leptons come from the heavy particle decay while in the first only one comes from the B and the other originates from the top quark. A cut on $p_T(L_1)$ will nevertheless be useful also for the B, but pushing it to too high values would induce a big unbalance between $T_{5/3}$ and B lowering the cross section too much for the latter. The p_T of the second lepton, which would not in any case solve this problem, turns out to be an inefficient cut because a hard cut on $p_T(L_1)$ already implies, on the background, a certain hardness of $p_T(L_2)$. This is the case, for instance, for the dominant $t\bar{t}$ background, and we therefore find it convenient to keep the cut on $p_T(L_2)$ to its minimal value of 10 GeV.

The essence of our signal is simply the decay of a heavy particle, whose energy needs to be distributed among its different products, leptons, jets (J), and $\not{E}_T$. It is therefore useful to define the total transverse energy H_T:

$$H_T = \sum_{J,L,\not{E}_T} |\vec{p}_T|. \tag{6}$$

The H_T distribution is shown in Fig. 4 and, as expected, peaks around the heavy particle mass. A cut on H_T will therefore be extremely useful and will also solve the problem of the unbalance among B and $T_{5/3}$ due to the $p_T(L_1)$ cut since H_T is typically bigger for B than for $T_{5/3}$. The reason why H_T is bigger for B is that $\not{E}_T$, which directly contributes to $\not{E}_T$, is also bigger and this is due to the following. The partner has, when singly produced, low transverse boost so that the $T_{5/3}$ decay products, the t and the W, are back to back in the transverse plane and boosted. This favors the two neutrinos from t and W to be

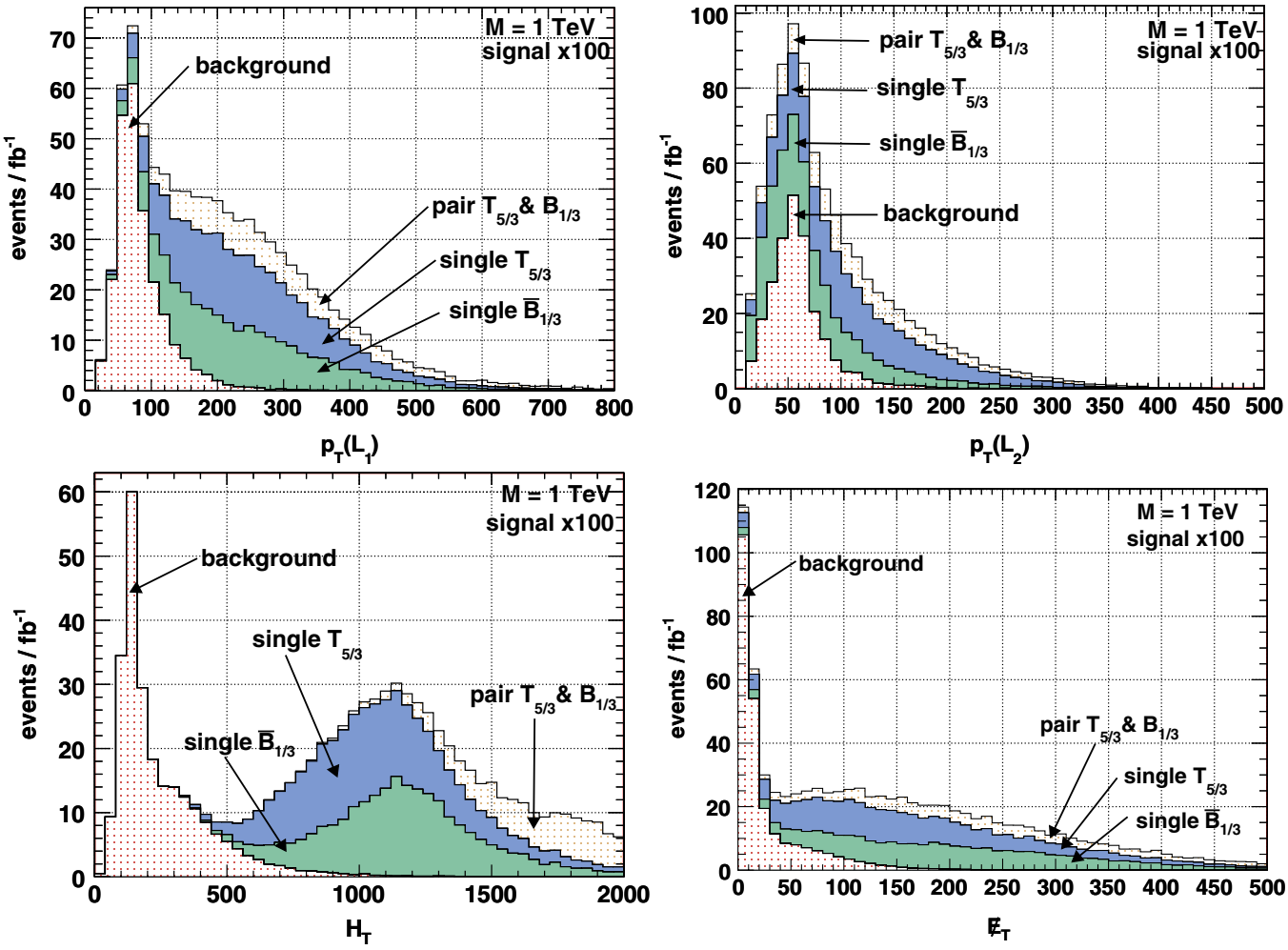

FIG. 4 (color online). Distribution of $p_T(L_1)$, $p_T(L_2)$, H_T, and $\not{E}_T$ for signal ($\times$ 100) and background after the minimal set of cuts, $p_T(L_{1,2} > 10)$ GeV, $M(LL) > 120$ GeV. The case $\lambda_{T,B} = 3$ is considered.

back to back, and in this configuration there is a cancellation in $\not{E}_T$. This cannot happen for the B where there is only one hard neutrino. It will nevertheless be hard, for masses $>$1.0 TeV, to balance the B and $T_{5/3}$ signals after cuts. The lepton-jet separation will indeed unavoidably disfavor the $T_{5/3}$ selection since it forbids too boosted leptonic tops.

The two main cuts we will use are, in conclusion, $p_T(L_1)$ and H_T, but we will also ask some $\not{E}_T$ and $M(LL) >$ 120 GeV as mentioned above to get rid of the $Z^*/\gamma*$ background. For different masses, we optimize our cuts for the case in which both the $T_{5/3}$ and B are present, have degenerate masses and "average" coupling $\lambda_{T,B} = 3$. The optimized values are shown in Table II, and the corresponding cross sections are reported in Table III. We define the discovery luminosity to be the one for which $S/\sqrt{B} =$ 5 or, if the background is negligible as in the 0.5 TeV mass case, as the luminosity which is needed to observe 5 signal events; the results are shown in Table IV. We see that discovery will be possible, in the degenerate mass case, up to at least 1.5 TeV top partner mass, while it appears difficult for 2 TeV even when the entire LHC program of 300 fb^{-1} total luminosity will be completed. For masses below around 1 TeV, moreover, even 100 fb^{-1} of luminosity will allow to collect a significant number (greater than 800) of signal events which will allow to study the top partners in some detail measuring their masses and couplings as we will discuss in the following section.

The situation is worst, clearly, when only the B partner is present. The discovery luminosity for different masses and

TABLE II. Table of the cuts depending on the mass of the partners. To these, there is a cut on the invariant mass of both leptons, $M(LL) > 120$ GeV, and the p_T of the second lepton, $p_T(L2) > 10$ GeV.

Cut	Mass, [TeV]	$p_T(L1)$, [GeV]	H_T, [GeV]	$\not{E}_T$, [GeV]
soft	0.5	60	500	50
medium	1.0	100	1000	50
hard	1.5	200	1200	100
max	2.0	250	1600	100

TABLE III. Cross section in [fb] for the different processes. For the signal, the mass corresponding to the cut is used.

	soft		medium		hard		max	
Process	++	−−	++	−−	++	−−	++	−−
Single $T_{5/3}$	38.4	18.7	1.50	0.64	0.154	0.059	0.015	0.005
Pair $T_{5/3}$	28.1	28.1	0.662	0.662	0.03	0.03	0.0021	0.0022
Single B	32.4	14.4	1.76	0.72	0.226	0.085	0.042	0.015
Pair B	26.3	26.3	0.651	0.651	0.03	0.03	0.0022	0.0022
True background	3.5	2.0	0.68	0.34	0.174	0.077	0.058	0.020
Sign background	12.3	12.3	0.72	0.72	0.100	0.100	0.009	0.009

for $\lambda_B = 3$ are shown in Table V after applying the cuts of Table II. Though the cuts are not optimized for this case, we see that the discovery is impossible for 2 TeV while the case of 1.5 TeV is within the reach of the LHC. Lowering the coupling renders the discovery more difficult for high mass, where the pair production is small, given that the single production cross section decreases as λ^2. For $\lambda_{T,B} = 2$ and degenerate masses, for instance, 90 fb^{-1} are needed for 1.5 TeV mass while the 2 TeV case is by far beyond reach. When only the B is present and $\lambda_B = 2$, the 1.0 case should be discovered with 11 fb^{-1}, while the 1.5 TeV case becomes difficult as the discovery luminosity, though again estimated with the cuts of Table II which are not optimized for this case, is of 287 fb^{-1}.

The top partners, even if both exist, need not to be degenerate or to have equal couplings. Actually, an unavoidable source of splitting is that, as discussed in Sec. II, the B mixes with the b_L while the $T_{5/3}$ does not. In the specific model described in Sec. II, this results in $M_B = M_Q/\cos\varphi_q$ while $M_T = M_Q$ which implies

$$\frac{M_T}{M_B} = \frac{\lambda_B}{\lambda_T} = \cos\varphi_q, \tag{7}$$

TABLE IV. Discovery luminosity, for different mass, in the case of degenerate top partners with $\lambda_{T,B} = 3$.

Mass, [TeV]	$L_{\text{discovery}}$, [fb^{-1}]	# signal	# background
0.5	0.024	5	0
1.0	1.103	8	2
1.5	26.40	17	11
2.0	326.7	28	31

TABLE V. Discovery luminosity, for different mass, when only the B partner is present and $\lambda_B = 3$.

Mass, [TeV]	$L_{\text{discovery}}$, [fb^{-1}]	# signal	# background
0.5	0.076	8	2
1.0	4.3	16	11
1.5	82	30	37
2.0	637	39	61

where φ_q is the mixing angle of the q_L doublet. Since the q_L will not be very composite to satisfy experimental constraints, i.e. $\sin\varphi_q$ is small, in our model the partners are likely to have similar masses, though the B will always be heavier than the $T_{5/3}$ and also more weakly coupled since $\lambda_B < \lambda_T$. The B cross section will therefore quickly decrease, especially for high masses where single production is more relevant, by increasing $\sin\varphi_q$, and a valid (although pessimistic) approximation of this case is to neglect the entire B partner contribution. This leads us to consider the case in which only the $T_{5/3}$ is present and $\lambda_T = 2$, which corresponds to maximal $\sin\varphi_q$. We obtain that the discovery is surely possible for 1 TeV mass, with 10 fb^{-1}, but it is very difficult for 1.5 TeV where 470 fb^{-1} would be needed. This case is worse than the one of the B since our cuts are, as we have explained, more efficient for the B than for the $T_{5/3}$ if $M_T > 1.0$ TeV. Even though discovery is difficult in this unfavorable situation for exactly 1.5 TeV mass, the cross section decreases so fast with the mass that already for 1.3 TeV discovery is possible, 90 fb^{-1} being required. Intermediate cases obeying Eq. (7) could also be considered, but we prefer not to restrict to the specific model of Sec. II and instead consider more general situations. Similar but not equal top partner masses and couplings will be considered in the following section where we will discuss the LHC phenomenology of the top partners in more detail.

Our event-selection strategy is also efficient for the pair production, as we have mentioned. If only pair production is considered, indeed, we find (when both partners are present) a discovery luminosity of 64 pb^{-1} and of 8.9 fb^{-1} for, respectively, 0.5 and 1.0 TeV mass, and this has to be compared with the values of 56 pb^{-1} and of 15 fb^{-1} which have been found in [21]. Since our background is larger, especially for low mass, due to the charge misidentification effect which was ignored in [21], our strategy seems more efficient.

IV. PHENOMENOLOGY OF THE TOP PARTNERS

The discovery of an excess in the same-sign dilepton channel would not be a proof of the existence of the top

partners since other new physics scenarios, or an erroneous estimate of the background cross section, could lead to the same effect. The aim of this section is to underline the main features of the top partner signal, which will be crucial for recognizing it, and also to propose some strategies for measuring the partner's masses and couplings. Since a large number of events is required to perform reliable measures, the results presented in this section are expected to be useful for masses below 1.2 or 1.3 TeV, the cross section likely to be too small in the 1.5 TeV case.

A. SM particles

Let us first of all try to identify the heavy SM particles, the W's and the hadronic top, which are present in our signal. This will already give us some confidence in the hypothesis that the dilepton excess is due to a modified charged current in the top sector, even though this feature is shared by the ttW and $ttWW$ backgrounds. Identifying the t will also help us later to reconstruct the new particles which would constitute the most striking evidence for their existence.

In our signal the leptons come from the decay of W bosons and even if this property is shared by most of the backgrounds, and is quite common for leptons in a hadronic environment, it is good to establish this fact in order to exclude, for instance, an exotic particle coupled to the charged lepton current such as a heavy W'. The presence of the W's in our signal, where the only sources of $\not{E}_T$ are the two neutrinos, is easily observable by the end point of the m_{T2} (also called stransverse mass) [34] distribution. This variable is designed to extract the mass M of a pair-produced particle with semi-invisible decay as shown in Fig. 5. It is defined as

$$m_{T2} = \min_{\vec{p}_T^1+\vec{p}_T^2=\vec{\not{p}}_T} \{\max_{i=1,2}\{m_T(\vec{p}_T^{\,i}, \vec{q}_T^{\,i})\}\} \leq M, \qquad (8)$$

where $\vec{\not{p}}_T$ is the $\not{E}_T$ vector and $\vec{q}_T^{\,i}$ are the transverse components of the visible part of the decay. In our case, $\vec{q}_T^{\,i}$ are the leptons transverse momenta and the m_{T2} distribution ends at m_W as shown in Fig. 6. It should be noted that when, as in our case, the transverse mass m_T in Eq. (8) is computed with massless particles (the lepton and the neutrino), m_{T2} will vanish if the neutrino momenta $\vec{p}_T^{\,1,2}$ can be chosen to be parallel and aligned with the leptons. This is always possible when the $\not{E}_T$ vector lays inside the angle between the lepton transverse momenta and, since our leptons are usually back to back, this will roughly happen one half of the times. The m_{T2} distribution therefore shows a peak at zero and, since the events in the peak are useless for determining the threshold, this effects reduces the efficiency of the procedure by a factor one half.

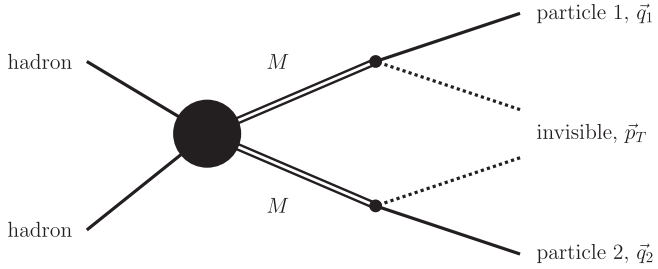

FIG. 5. Topology for which m_{T2} is defined: pair production of particle with semi-invisible decay.

The signal also contains a hadronic top which we can reconstruct in two steps. First, we reconstruct the hadronic W and afterwards we associate to it the corresponding jet from the top decay. The latter will be a b jet, but b tagging will not be needed. Except for single production of $T_{5/3}$, the top will be slightly boosted since it comes from the decay of a heavy particle, as shown in Fig. 7. The W and the b will still be separated enough to be resolved while the two W jets have a certain probability (we use a cone jet with $\Delta R = 0.7$ and $\not{E}_{T\,\mathrm{min}} = 20$ GeV) to merge into a single jet, as Fig. 7 shows. We therefore proceed as follows. First, we look for a single jet with $|m(J) - m_W| \leq 20$ GeV and if none is found, we do the same with all the jet pairs $|m(J_1 + J_2) - m_W| \leq 20$ GeV. To each W reconstructed in this way, we try to associate a jet such that $|m(W + J) - m_t| \leq 30$ GeV and when this is achieved the top is considered to be reconstructed. For the signal, we estimate the efficiency of this procedure to be above 60%, even though a detailed detector simulation would be needed for a more detailed identification and hence a realistic estimate.

B. Evidences of single production

If the top partners coupling to top is large, as theoretically expected, a sizable fraction (or even the entire sample, for high mass) of the dilepton events originates from single production, and establishing this fact will permit us to distinguish the top partner from a generic pair-produced

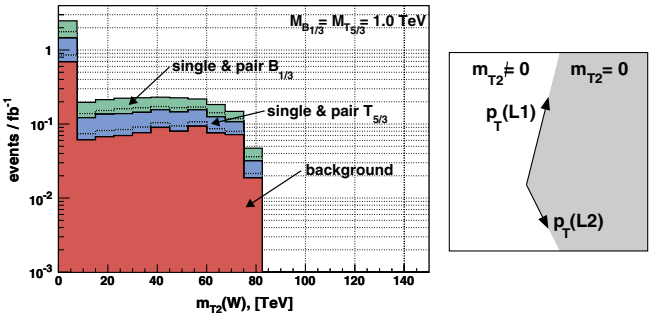

FIG. 6 (color online). On the left, m_{T2} distribution for the signal with $M_T = M_B = 1.0$ TeV, $\lambda_{T,B} = 3$ selecting only the l^+l^+ final state. The large peak at $m_{T2} = 0$ is due to configurations in which the lepton and neutrino transverse momenta could be parallel, which is the case when the $\not{E}_T$ vector falls in the red region shown on the right.

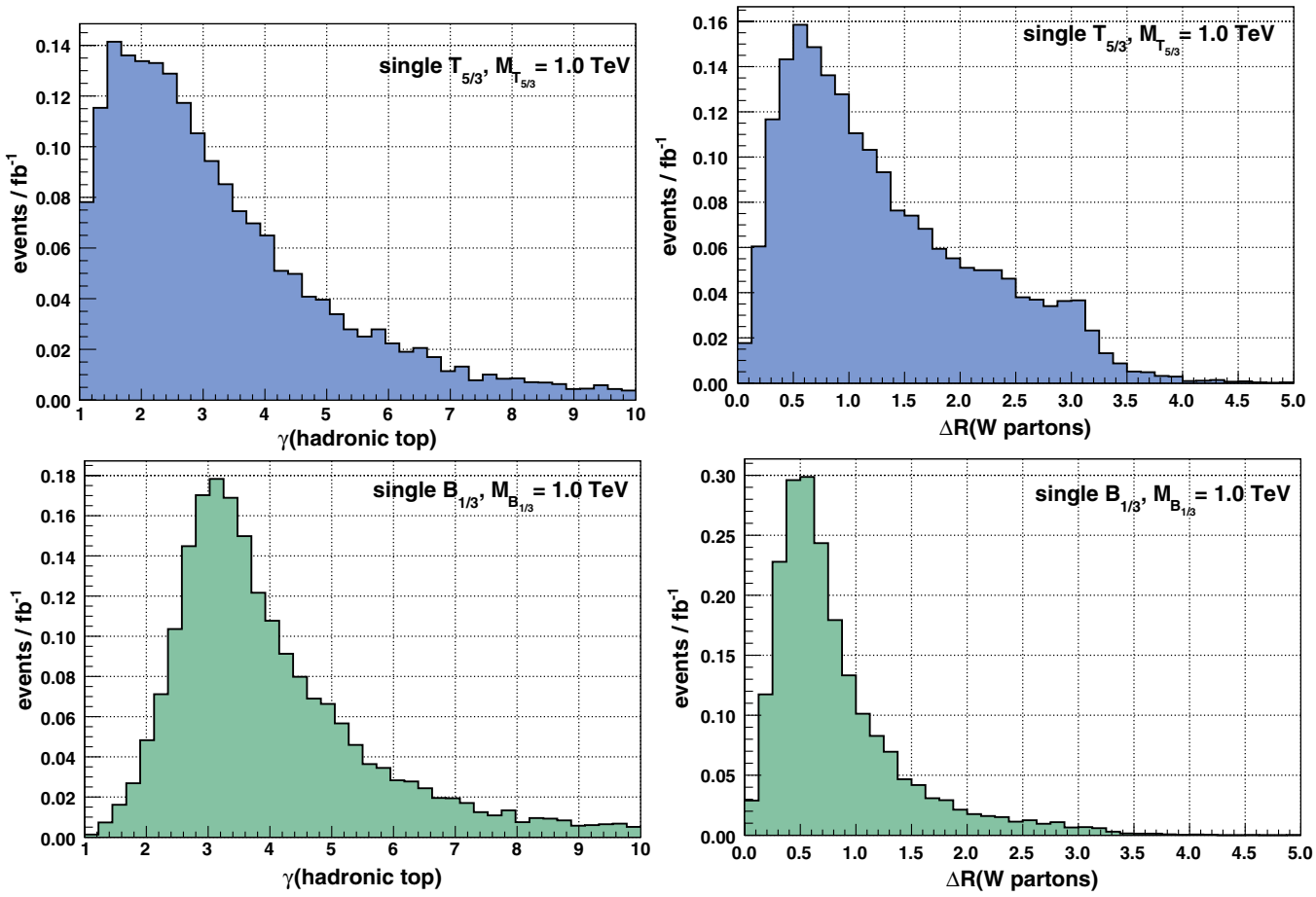

FIG. 7 (color online). The left plots show the Lorentz factor γ of the hadronic top for $T_{5/3}$ and B, while the right plots shows the ΔR separation of the partons originating from the W decay. Signal events are used with $M_{T,B} = 1.0$ TeV, $\lambda_{T,B} = 3$, and "medium" cuts are applied.

new heavy colored fermion. Studying single production will also allow us to measure the top partners coupling.

The first evidence of single production is the presence of a charge asymmetry which is due, as discussed in Sec. III, to the fact that the single production originates from a W radiated by an initial quark which, because of the high energy needed, will most of the time be a valence quark (90% of ug initial partons for $M = 1.0$ TeV with l^+l^+ final state). The difference in the $(++)$ and $(--)$ cross section is shown in Fig. 8 for $M_{T,B} = 0.5$–1.5 TeV and $\lambda_{T,B} = 2, 3, 4$. The difference in the cross sections, rather than the asymmetry, could be a better observable in our case because the sign background contribution, as well as the one from pair production, disappears. In the asymmetry, it enters in the denominator. For known M_T and M_B, the charge asymmetry will put a constraint on the $\lambda_{T,B}$ couplings; we will come back on this later.

The presence of a forward energetic jet is, as we have discussed in Sec. III, additional evidence of the single production. Initial state radiation (ISR) in the pair production signal or in the background, when constrained by our cuts to kinematical regions of high hard scale, produces forward jets which are similar to the one we want to observe. The ISR jets are the main background to the

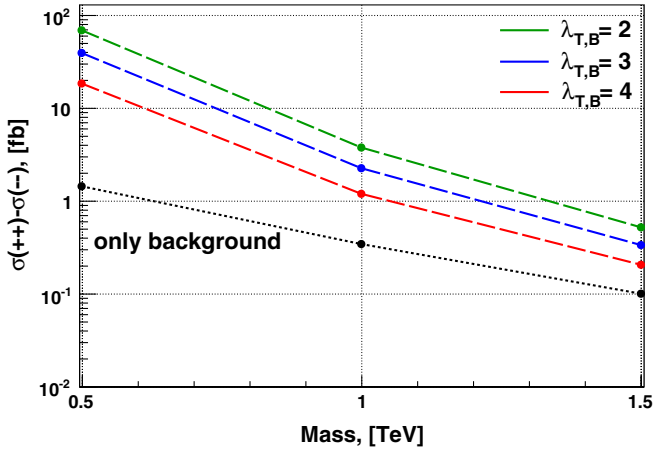

FIG. 8 (color online). The cross-section difference $\sigma(++) - \sigma(--)$, at different masses, of signal + background for different values of $\lambda_{T,B} = 2, 3, 4$. For each mass, the corresponding set of cuts is used.

forward jet identification, and it is therefore important to take this effect into account. Figure 9 shows the typical ISR distribution for a hard scale of 2 TeV in the p_T-η plane and in the jet energy. Compared with the signal (see again Fig. 9), the ISR jets distribution is peaked around softer and more central emissions even for very hard (2 TeV) processes. For technical reasons, we have obtained the ISR radiation distribution in Fig. 9 by simulating the Drell-Yan production of a Z' boson of 2 TeV mass. This allowed us to obtain quickly large samples of high hard scale events and therefore a readable two-dimensional distribution, while the resulting shapes are independent of this technicality. Figure 9 suggests the following criteria to identify the forward jet. First, it has to be energetic, $E > 300$ GeV, but this will also be often true for the other hard jets of our signal and background. Among these candidates, we therefore look for low p_T and forward jets by imposing $p_T < 150$ GeV and $\eta > 2.5$. In case of multiple candidates, we take the most energetic one. The efficiency on the single production at 1.0 TeV is 65%, while the fake forward jet probability from the backgrounds and pair production is around 20%. Most of these fakes, as we have explained, come from the ISR effects which are of course included in our simulation of the background and of the pair production.

C. Identification of the top partners

The evidence for the top partners discussed up until now is indirect, and we will now try to identify the particles responsible for the excess, which would provide a direct proof of their existence. In what follows, we will propose a method to detect the presence of the $T_{5/3}$ and/or of the B particles and to extract their mass. If one of them is significantly lighter than the other, or more strongly coupled, it will appear as the only particle present.

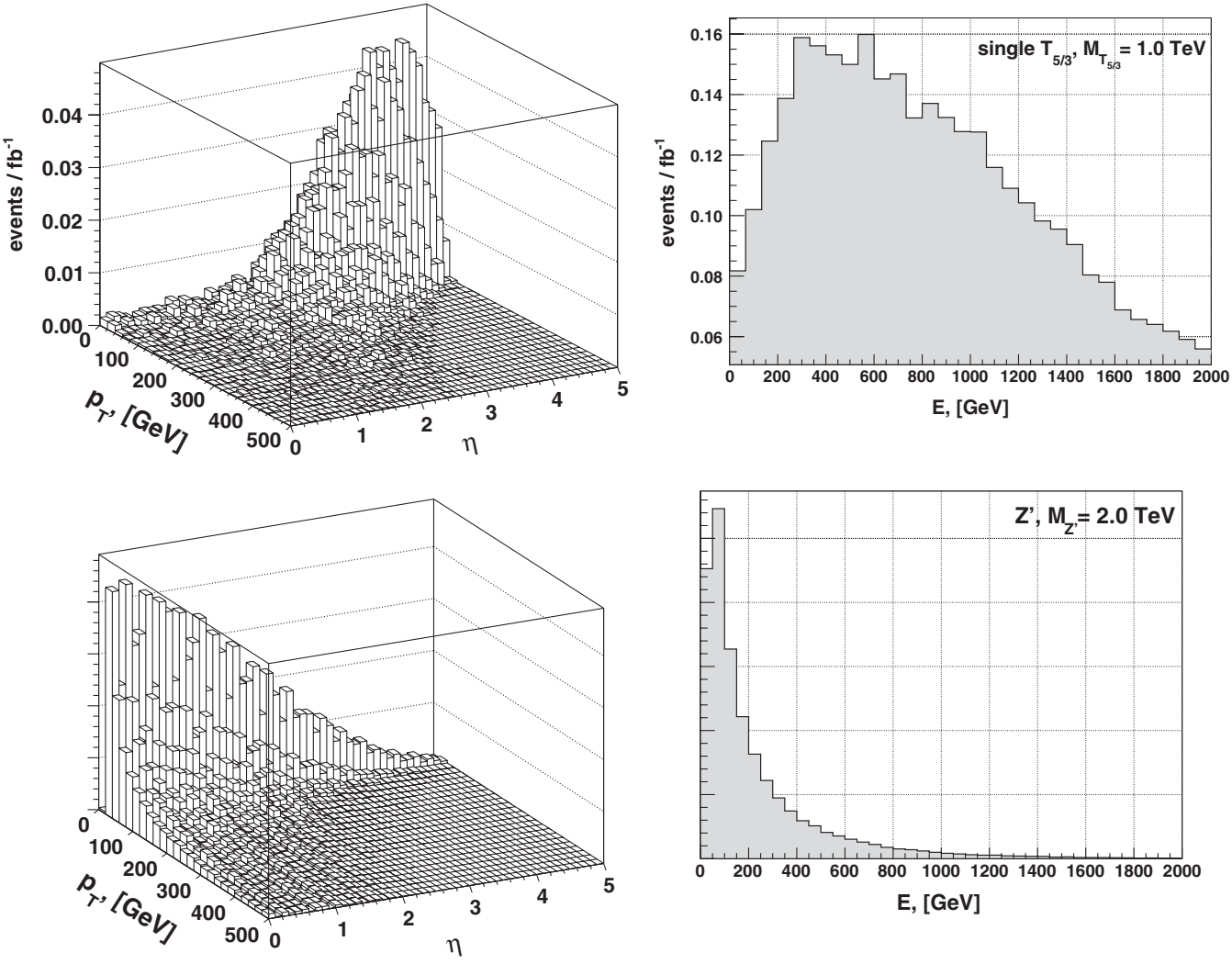

FIG. 9. Distribution in the $p_T - \eta$ (left) plane and in energy (right) of the signal forward jet (top) and of the ISR jets (bottom). The signal is for single $T_{5/3}$ ($M_T = 1.0$ TeV, $\lambda_T = 3$) production, while ISR was simulated with a 2 TeV Z'.

Otherwise, our signal will contain a mixture of the two charges whose relative importance depends on the masses and on the couplings.

1. Charge

We would like first of all to establish whether our signal can originate from a heavy fermion with charge $-1/3$ (the B), $+5/3$ (the $T_{5/3}$) or from a combined contribution of both. We will make use of the fact that (see Fig. 1) both leptons come from the partner decay in the case of the $T_{5/3}$, while the second lepton comes from the other top (or B) leg in the case of the B. This will be used in different ways, depending on the mass. For low masses, $M_{T,B} = 0.5$ TeV, the partners will be boosted along the beam axis (see Fig. 10) and when this is the case their decay products tend to be aligned and in the forward region. This is inherited, in the case of the $T_{5/3}$, by the two leptons, which therefore are preferentially emitted in the same hemisphere. The opposite happens when the $T_{5/3}$ is at rest since its decay products tend to be back to back in this case. This makes, as shown in Fig. 11, that the angle $\theta(L_2)$ of the second (in p_T) lepton with the beam, having oriented the system in such a way that $\theta(L_1) < \pi/2$, peaks at small values when the $T_{5/3}$ is boosted and at large values when it is at rest. The $T_{5/3}$ being preferentially boosted for 0.5 TeV, the total distribution shows a preference for aligned leptons and, since this feature is not present in the case of the B, in can be used to distinguish the two. We therefore define the asymmetry between the events in which both leptons are in

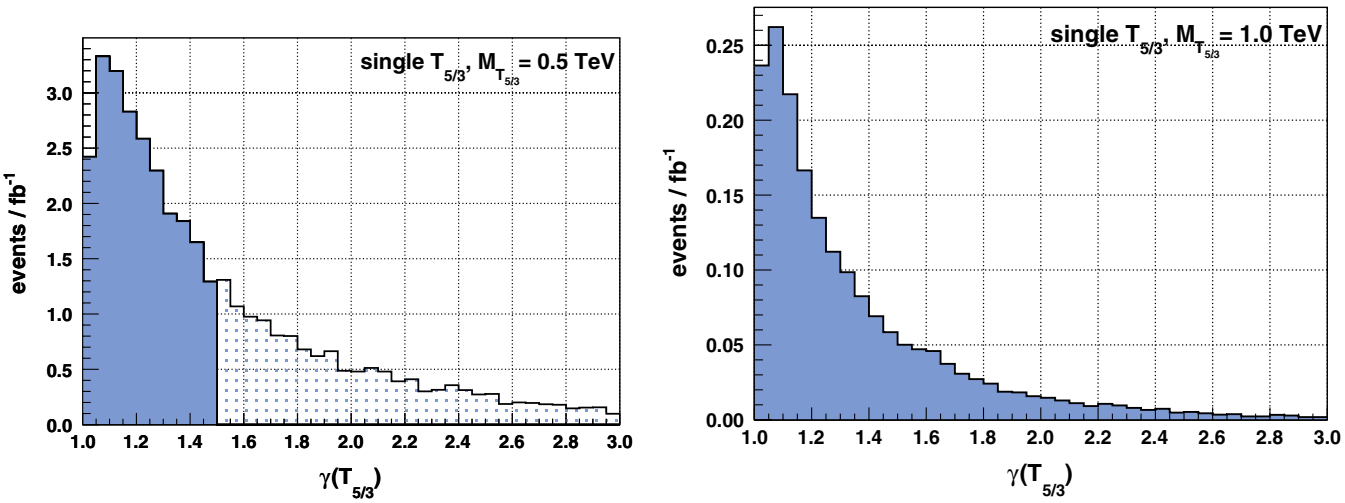

FIG. 10 (color online). The γ factor for $T_{5/3}$ in the case $M_T = 0.5$ TeV or 1.0 TeV. The sample is divided into two bins: shaded for $\gamma > 1.5$ and plain for $\gamma < 1.5$.

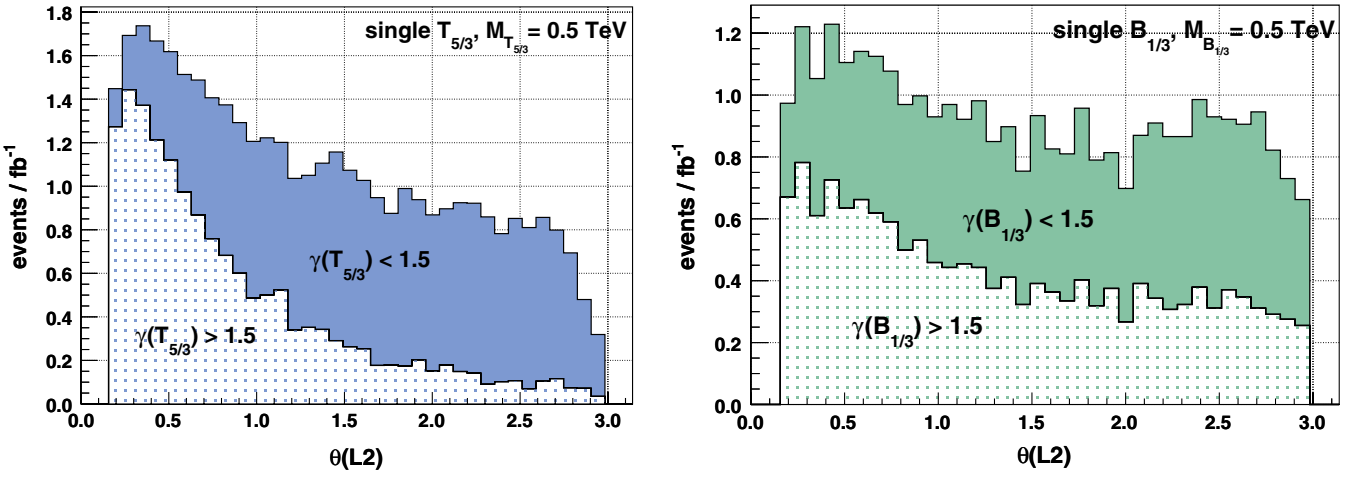

FIG. 11 (color online). The angle with the beam of the second lepton ($\theta(L2)$) for $T_{5/3}$ and B, $M_{T,B} = 0.5$ TeV. The system is always oriented to have $\theta(L1) < \pi/2$. We see that boosted $T_{5/3}$ leads to aligned leptons in the forward region, while if it is at rest the leptons tend to be opposite. The distribution is more symmetric in the case of the B.

TABLE VI. Table giving the asymmetry between leptons in same or opposite hemisphere, $A_{ll}^{\text{hemisphere}}$, for the signal (single and pair production) at $M_T = M_B = 0.5$ TeV with soft cuts applied. The background contribution is negligible for low masses, therefore it has been ignored.

	$A_{ll}^{\text{hemisphere}}$
$T_{5/3}$	0.23
B	0.05
$T_{5/3} + B$	0.14

TABLE VII. Table giving $R_{ll}^{\Delta\varphi} = (\#\Delta\varphi_{ll} > 2.5)/(\#\Delta\varphi_{ll} < 1.0)$ for $M_T = M_B = 1.0$ TeV, with medium cuts applied. Significantly different results are obtained in the various configurations with only the $T_{5/3}$, only the B or a superimposition of the two.

	$R_{ll}^{\Delta\varphi}$
background	2.95
$T_{5/3}$ + background	6.00
B + background	1.98
$T_{5/3} + B$ + background	3.33

the same or opposite hemispheres ($\theta \lessgtr \pi/2$), $A_{ll}^{\text{hemisphere}} = (\#\text{same} - \#\text{opposite})/(\#\text{all})$. The predicted asymmetry for B, $T_{5/3}$ and for a combination of the two are shown in Table VI; we observe significantly different results in the various cases.

For higher masses, $M_{T,B} \gtrsim 1.0$ TeV, the partners will hardly be boosted and the hemisphere asymmetry will be washed out. To distinguish the $T_{5/3}$ from the B, we can use, in this case, the fact that the partners usually have very small transverse boost as a result of the single production mechanism. Moreover, since they are heavy, the top and the W from their decay will be significantly boosted so that they will transmit their direction to their decay product. In the case of $T_{5/3}$, therefore, the leptons will preferentially be back to back in the transverse plane, as shown in Fig. 12. Notice that the leptons tend to be separated in the transverse plane also for the B, due to the fact that the B and the leptonic top in the single production diagram preferentially go in opposite transverse directions. This feature is however less sharp for the B and can be used for the identification of the partners. The ratio between opposite lepton pairs and the aligned ones, $R_{ll}^{\Delta\varphi} = (\#\Delta\varphi_{ll} > 2.5)/(\#\Delta\varphi_{ll} < 1.0)$, is reported in Table VII and seems a promising observable to distinguish among the partners.

2. Mass

Let us now discuss some strategies to measure the top partners mass. The first method that could be employed is based on the "m_{T2}-assisted" missing momenta reconstruction proposed in [35], which is suited for our case since the only sources of $\not{E}_T$ are the two neutrinos from the W decays. This is based on the possibility of reconstructing the neutrino's momenta, and therefore also the $W's$, in the events which lie close to the m_W threshold of the m_{T2} distribution of Fig. 6, and once these are known the top partners could be reconstructed both in the single and pair production cases (see Fig. 1) by reconstructing their decay products. In all cases we need to identify a b quark not belonging to a hadronic top, and for the B we also need to establish which of the reconstructed W originates from a semileptonic top. This could be achieved by requiring the $b + W$ invariant mass to be close to m_t. We will not study this interesting possibility in detail, but we will rather describe other methods to measure the top partner mass based on more standard observables.

For the $T_{5/3}$, two strategies can be employed. If it is pair produced, the $T_{5/3}$ which produces the leptons is accompanied by a second $T_{5/3}$ with hadronic decay (see Fig. 1).

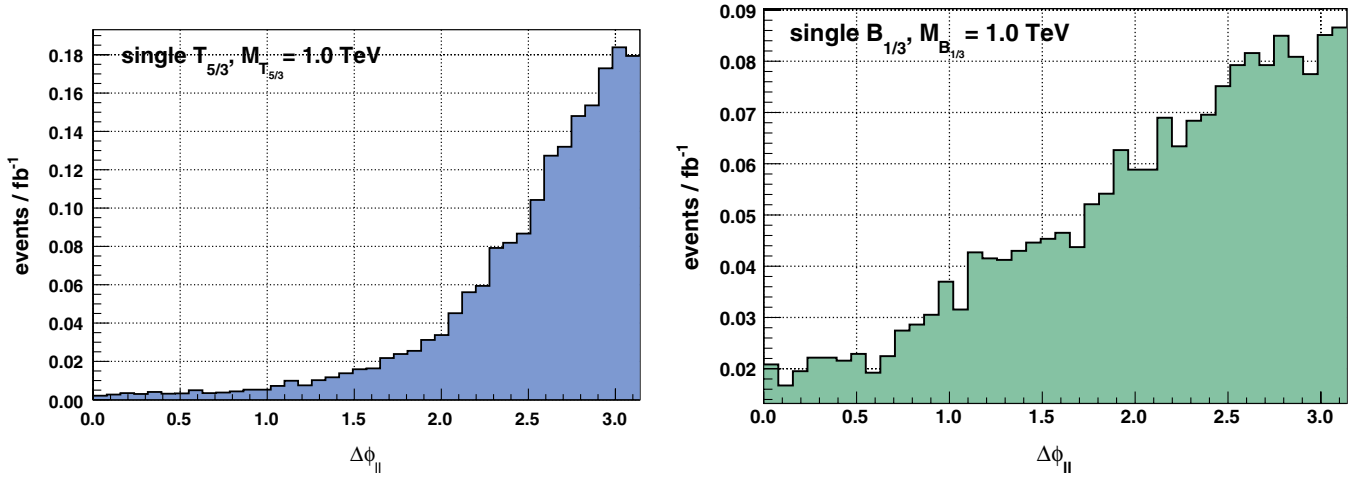

FIG. 12 (color online). $\Delta\varphi(LL)$ for $T_{5/3}$ and B, $M_T = M_B = 1.0$ TeV, medium cuts. The heavy particle tends to have low p_T; for the $T_{5/3}$, this will imply that the leptons are back to back in the transverse plane as can be seen in the left plot. For the B, one lepton comes from its decay while the other comes from the opposite top leg; their azimuthal angles are therefore less correlated.

The latter can be reconstructed and its mass measured as proposed in [21]. A second method, not based on pair production and therefore suited also for high masses where the pair production cross section is low, is based on the usual transverse mass m_T [36], extended to more than two particles

$$m_T = \sqrt{\left(\sum_i p_{Ti}\right)^2 - \left(\sum_i \vec{p}_{Ti}\right)^2}, \tag{9}$$

where the sum will run over $i = \not{E}_T, L_1, L_2, b$, the b being defined as a b jet (identified with an efficiency of $\epsilon_b \approx 0.5$) not belonging to the hadronic top. Our m_T is an underestimate of the true $T_{5/3}$ transverse mass, since the sum of the neutrinos' transverse energies has been replaced with $\not{E}_T = |\vec{\not{E}}_T| = |\vec{p}_T(\nu_1) + \vec{p}_T(\nu_2)| \leq |\vec{p}_T(\nu_1)| + |\vec{p}_T(\nu_2)|$. The central relation $m_T < M_T$ is therefore satisfied, and we can use the end point of the m_T distribution to measure the $T_{5/3}$ mass. The main background which affects this distribution is the other partner; we can however obtain a cleaner sample of $T_{5/3}$ events by the cut $\Delta\varphi_{ll} > 2.5$ (see Fig. 12). We will describe a concrete example of this method in the following subsection.

In the case of the B, and for single production, we can use the m_{T2} variable introduced above ([Eq. (8)], but in a

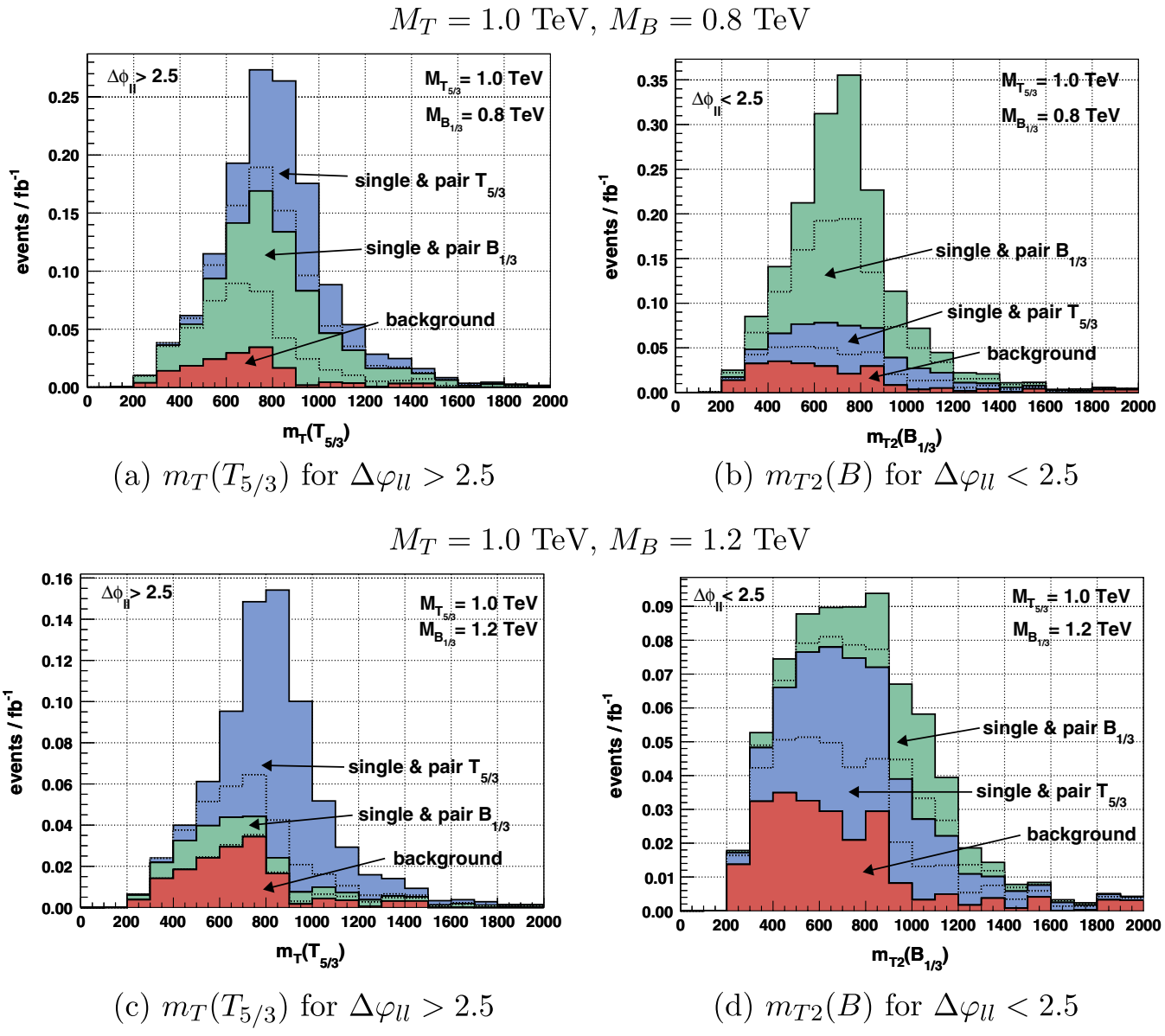

FIG. 13 (color online). $m_T(T_{5/3})$ and $m_{T2}(B)$ distributions constructed as defined in the text, with, respectively, $\Delta\varphi_{ll} \gtrless 2.5$. These plots show the results only for the l^+l^+ channel after medium cuts. b tagging efficiency is taken into account. We notice how well the $\Delta\varphi_{ll}$ selection works. For the $m_T(T_{5/3})$, we look for a peak followed by a threshold at M_T, while for $m_{T2}(B)$ we observe for a sharp decrease at M_B. It seems that all masses could be extracted.

nonstandard way since we will apply it to a system of nondegenerate particles, the B and the leptonic top (see Fig. 1). To assign each lepton to the right leg, we will use that the one coming from the decay of the B will often be the hardest one (for $M_B = 1.0$ TeV this is true the 83% of the cases). The hardest lepton will therefore be combined with the hadronic top, reconstructed as discussed above, and which constitutes the first visible decay product. Therefore, in the notation of Eq. (8), we have $q_1 = p(L1) + p(\text{hadronic top})$. For the second particle, we require a b jet (paying again an efficiency $\epsilon_b \approx 0.5$) and we combine it with the second lepton: $q_2 = p(L2) + p(b)$. The end point of the m_{T2} distribution is the heaviest of the two decaying particles, namely M_B. The biggest background for the M_B determination is the $T_{5/3}$ contribution, which can be lowered by selecting events with $\Delta\varphi_{ll} < 2.5$; see Fig. 12.

3. Example

The methods described in this section should allow us to easily distinguish the situations in which only the B or only the $T_{5/3}$ are present, and to measure their mass. In order to test our ability to disentangle the B and $T_{5/3}$ effects in more subtle situations, we consider now the case in which $M_T = 1.0$ TeV and $M_B = 0.8(1.2)$ TeV and $\lambda_{T,B} = 3$. We will see that the identification of the two particles is more difficult but still possible. The total cross section after cuts for the signal is 12.2 fb (5.0 fb), while for the background we have 2.5 fb, which leads to $L_{\text{disc}} = 490$ pb^{-1} (2.4 fb^{-1}). The different mass distributions are shown in Fig. 13, and they indicate that it should be possible to extract the mass of both exotic quarks even in these intermediate situations by using the different transverse semileptonic mass distributions defined above.

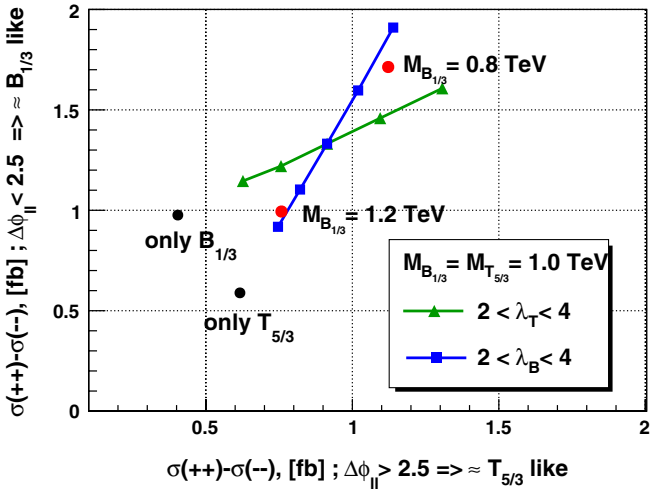

FIG. 14 (color online). Charge asymmetry for events with $\Delta\varphi_{ll} > 2.5$ (rather $T_{5/3}$-like) and $\Delta\varphi_{ll} < 2.5$ (rather B-like), for $M_T = M_B = 1.0$ TeV and varying λ_T, λ_B. The bigger λ, the larger asymmetry since single production is enhanced. The two points with only $T_{5/3}$ or B with $\lambda_{B,T} = 3$, and the two points with different values of M_B, described in the example above, are also shown. We see that these two variables have distinct dependence in λ_T, λ_B and could therefore in principle be inverted to measure them independently.

4. Coupling constants

If only one partner is present, then its nature could be established and its mass measured in the way we have discussed. Once this is done, its coupling constant could be extracted from the charge asymmetry; see Fig. 8. When both partners are present, we will still be able to measure their mass, but even when the latter is known one more observable will be needed, on top of the charge asymmetry, to measure their couplings. One possible strategy would be to measure the charge asymmetry (or better, the cross-section difference) for the two sets of events with $\Delta\varphi_{ll} \lessgtr 2.5$. Since we have already seen that the transverse angular separation is (for MT, $B \sim 1.0$ TeV, at least) an efficient criterion for separating the two contributions, the two observables will show different sensitivities to λ_T and to λ_B. This is shown in Fig. 14.

V. LOWER BEAM ENERGY

In our analysis we have assumed the LHC to work at its design center-of-mass energy of $\sqrt{S} = 14$ TeV, and there is no reason to doubt that this energy will be reached at some stage of the LHC program. It is known, however, that the program will start with lower beam energies, so that it is worth discussing how our result will be modified in that case. Two mechanisms are at work when lowering the beam energy. First, all of the cross sections scale down, but those with a high intrinsic scale decrease faster, as Fig. 15 shows. For instance, while single $B(1.0\ \text{TeV})$ goes down by a factor ≈ 4.0, $t\bar{t}$ only decreases of a factor ≈ 2.3 for $\sqrt{s} = 14 \rightarrow 10$ TeV. Second, since our cuts are only based on the hard transverse dynamics resulting from the decay of the partners, their efficiency on the signal will only depend on the mass and not on the beam energy. For the background, on the contrary, the efficiency of the cuts decreases with the beam energy since hard background events which could pass the cuts become less frequent. As an example, medium cuts on tt have an efficiency of $2.6 \cdot 10^{-2}$ at 14 TeV and of $1.7 \cdot 10^{-2}$ at 10 TeV.

It is therefore not worth modifying the cuts for lower energies. The discovery luminosities at 10 TeV energy in the case $M_B = M_T$ and $\lambda_{T,B} = 3$, presented in Table VIII, are obtained with the same cuts discussed in Sec. III. The table shows that for $M_B = M_T = 0.5$ or 1.0 TeV, the discovery will be relatively easy, and that even for $M_B = M_T = 1.5$ TeV, discovery will be possible if the entire programmed luminosity of 300 fb^{-1} will be collected at this energy.

Under the assumption that enough luminosity will be collected, the phenomenological study of the top partners

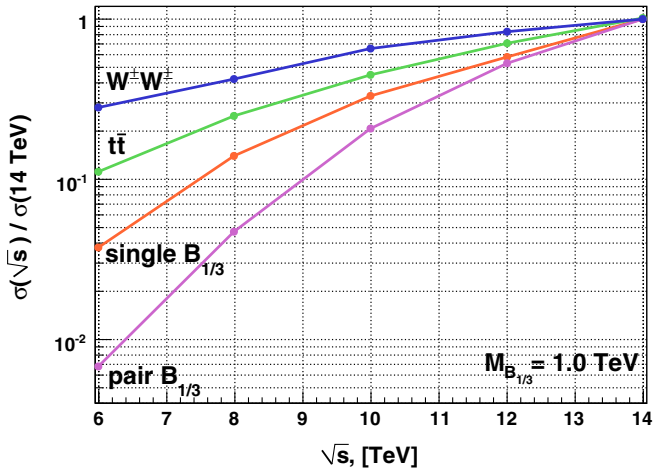

FIG. 15 (color online). Dependence on the beam energy of the cross section for single and pair B ($M_B = 1.0$ TeV), $t\bar{t}$, and $W^{\pm}W^{\pm}$. They are normalized to their 14 TeV value. We observe that the higher the intrinsic scale is, the more it is suppressed at low beam energy.

and the measure of couplings and masses will still be possible; we have checked that the discussion of Sec. IV is still valid, for 10 TeV energy, with minor numerical modifications.

VI. CONCLUSIONS

We have studied the possibility of observing heavy partners of the top quark at the LHC, in the channel of same-sign dileptons. The top partners constitute a robust consequence of the partial compositeness hypothesis, which is realized in the compelling 5D (or 5D-inspired) models of strong-sector EWSB. We have seen that, under wide and motivated assumptions, the top partners are expected to couple strongly to the top quark through a vertex which also contains a longitudinal W boson, and that this vertex is responsible for a sizable single production cross section. The latter dominates, for high top partner mass, over the QCD-mediated pair production and therefore extends the discovery reach of the LHC. We have found that the discovery will be possible up to at least 1.5 TeV in almost the entire expected parameter space.

Top partners below 1.5 TeV, as discussed in the Introduction, are very likely to be present in both the Higgsless and in the composite-Higgs scenarios, so that the one of same-sign dileptons is found to be a very promising channel in which these models could be tested at the LHC. For the composite-Higgs case, in which all other new states are expected to be heavier than the top partners which lie in the [0.5, 1.5] TeV range, the signal we have studied could constitute the most accessible experimental prediction.

TABLE VIII. Cross sections and discovery luminosity for $M_B = M_T = 0.5$, 1.0 and 1.5 TeV, with a beam energy at 10 TeV. The cuts used are the same as at 14 TeV, which leads to similar signal over background and hence lower significance. They are nevertheless still relevant.

Mass, [TeV]	σ, [fb]		$L_{\text{discovery}}$, [fb^{-1}]	# events	
	signal	background		signal	background
0.5	69.8	10.9	0.072	5	0
1.0	1.64	0.65	5.5	9	3
1.5	0.11	0.092	210.0	22	19

We have also discussed how, after the discovery of an excess, the presence of the top partners could be detected and their masses and couplings measured. Single production plays, also in this case, a major role since it allows us to distinguish the partners from generic colored heavy fermions and to measure their couplings.

The above results have been established by performing a quite detailed simulation, using the MADGRAPH/MADEVENT tools with showering performed with PYTHIA and the emission of extra partons taken into account by the MLM matching prescription. However, no genuine higher order corrections have been taken into account while these are expected to be sizable [37] both for the signal and for the background. Also, we have not included detector effects apart from charge misidentification and fake $\not{E}_T$. A more detailed analysis, for which we hope our results constitute a valid starting point, should clearly include a full detector simulation and the above-mentioned radiative corrections should be taken into account.

ACKNOWLEDGMENTS

We are indebted to R. Contino, R. Franceschini, and especially R. Rattazzi for many useful discussions and suggestions. We thank M. Pierini for instructive conversations and especially for pointing out to us the usefulness of the m_{T2} variable in our context. We also acknowledge L. Fiorini, S. Frixione, and M. Volpi for discussions. This work was supported by the Swiss National Science Foundation under Contract No. 200021-116372.

[1] L. Randall and R. Sundrum, Phys. Rev. Lett. **83**, 3370 (1999).
[2] S. Weinberg, Phys. Rev. D **13**, 974 (1976).
[3] M. J. Dugan, H. Georgi, and D. B. Kaplan, Nucl. Phys. **B254**, 299 (1985).
[4] C. Csaki, C. Grojean, H. Murayama, L. Pilo, and J.

Terning, Phys. Rev. D **69**, 055006 (2004); C. Csaki, C. Grojean, L. Pilo, and J. Terning, Phys. Rev. Lett. **92**, 101802 (2004); C. Csaki, C. Grojean, J. Hubisz, Y. Shirman, and J. Terning, Phys. Rev. D **70**, 015012 (2004); G. Cacciapaglia, C. Csaki, C. Grojean, and J. Terning, Phys. Rev. D **71**, 035015 (2005); K. Agashe, C. Csaki, C. Grojean, and M. Reece, J. High Energy Phys. 12 (2007) 003.

[5] G. Cacciapaglia, C. Csaki, G. Marandella, and J. Terning, Phys. Rev. D **75**, 015003 (2007).

[6] R. S. Chivukula *et al.*, Phys. Rev. D **74**, 075011 (2006); S. Matsuzaki, R. S. Chivukula, E. H. Simmons, and M. Tanabashi, Phys. Rev. D **75**, 073002 (2007); H.-J. He *et al.*, Phys. Rev. D **78**, 031701 (2008).

[7] R. Contino, Y. Nomura, and A. Pomarol, Nucl. Phys. **B671**, 148 (2003); K. Agashe, R. Contino, and A. Pomarol, Nucl. Phys. **B719**, 165 (2005).

[8] R. Contino, L. Da Rold, and A. Pomarol, Phys. Rev. D **75**, 055014 (2007).

[9] D. B. Kaplan, Nucl. Phys. **B365**, 259 (1991).

[10] R. Contino and A. Pomarol, J. High Energy Phys. 11 (2004) 058.

[11] R. Contino, T. Kramer, M. Son, and R. Sundrum, J. High Energy Phys. 05 (2007) 074.

[12] T. Gherghetta and A. Pomarol, Nucl. Phys. **B586**, 141 (2000).

[13] C. Csaki, A. Falkowski, and A. Weiler, J. High Energy Phys. 09 (2008) 008.

[14] K. Kumar, T. M. P. Tait, and R. Vega-Morales, J. High Energy Phys. 05 (2009) 022; A. Pomarol and J. Serra, Phys. Rev. D **78**, 074026 (2008).

[15] B. Lillie, L. Randall, and L.-T. Wang, J. High Energy Phys. 09 (2007) 074; K. Agashe, A. Belyaev, T. Krupovnickas, G. Perez, and J. Virzi, Phys. Rev. D **77**, 015003 (2008); G. H. Brooijmans *et al.*, arXiv:0802.3715.

[16] A. Birkedal, K. Matchev, and M. Perelstein, Phys. Rev. Lett. **94**, 191803 (2005); K. Agashe *et al.*, arXiv:0810.1497.

[17] M. S. Carena, E. Ponton, J. Santiago, and C. E. M. Wagner, Phys. Rev. D **76**, 035006 (2007); R. Barbieri, B. Bellazzini, V. S. Rychkov, and A. Varagnolo, Phys. Rev. D **76**, 115008 (2007); M. Gillioz, Phys. Rev. D **80**, 055003 (2009); C. Anastasiou, E. Furlan, and J. Santiago, arXiv:0901.2117.

[18] G. F. Giudice, C. Grojean, A. Pomarol, and R. Rattazzi, J. High Energy Phys. 06 (2007) 045; R. Contino, C. Grojean, M. Moretti, F. Piccinini, and R. Rattazzi, arXiv:1002.1011.K. Cheung, C.-W. Chiang, and T.-C. Yuan, Phys. Rev. D **78**, 051701 (2008).

[19] A. Atre, M. Carena, T. Han, and J. Santiago, Phys. Rev. D **79**, 054018 (2009); J. A. Aguilar-Saavedra, Phys. Lett. B **625**, 234 (2005); J. High Energy Phys. 11 (2009) 030; G. Azuelos *et al.*, Eur. Phys. J. C **39S2**, 13 (2005); C. Dennis, M Karagoz Unel, G. Servant, and J. Tseng, arXiv:hep-ph/0701158; W. Skiba and D. Tucker-Smith, Phys. Rev. D **75**, 115010 (2007); M. Carena, A. D. Medina, B. Panes, N. R. Shah, and C. E. M. Wagner, Phys. Rev. D **77**, 076003 (2008); T. Bose and M. Narain, CERN Report No. CERN-CMS-CR-2008-005, 2008; J. A. Aguilar-Saavedra, Proc. Sci., TOP2006 (2006) 003.

[20] T. Han, H. E. Logan, B. McElrath, and L.-T. Wang, Phys. Rev. D **67**, 095004 (2003); M. Perelstein, M. E. Peskin, and A. Pierce, Phys. Rev. D **69**, 075002 (2004).

[21] R. Contino and G. Servant, J. High Energy Phys. 06 (2008) 026.

[22] M. S. Carena, E. Ponton, J. Santiago, and C. E. M. Wagner, Nucl. Phys. **B759**, 202 (2006); A. D. Medina, N. R. Shah, and C. E. M. Wagner, Phys. Rev. D **76**, 095010 (2007); G. Cacciapaglia, C. Csaki, G. Marandella, and J. Terning, J. High Energy Phys. 02 (2007) 036; G. Panico, E. Ponton, J. Santiago, and M. Serone, Phys. Rev. D **77**, 115012 (2008).

[23] K. Agashe, R. Contino, L. Da Rold, and A. Pomarol, Phys. Lett. B **641**, 62 (2006).

[24] S. S. D. Willenbrock and D. A. Dicus, Phys. Rev. D **34**, 155 (1986).

[25] A. D. Martin, W. J. Stirling, R. S. Thorne, and G. Watt, Eur. Phys. J. C **63**, 189 (2009); Eur. Phys. J. C **64**, 653 (2009).

[26] R. N. Cahn and S. Dawson, Phys. Lett. **136B**, 196 (1984).

[27] G. L. Bayatian *et al.*, CERN Report No. CERN-LHCC-2006-001, 2006; G. Aad *et al.*, arXiv:0901.0512; CERN Report No. CERN-LHCC-99-14, Vol. 1, 1999.

[28] J. Alwall *et al.*, J. High Energy Phys. 09 (2007) 028.

[29] T. Sjostrand, S. Mrenna, and P. Skands, J. High Energy Phys. 05 (2006) 026.

[30] S. Catani, F. Krauss, R. Kuhn, and B. R. Webber, J. High Energy Phys. 11 (2001) 063.

[31] J. Alwall *et al.*, Eur. Phys. J. C **53**, 473 (2008).

[32] M. L. Mangano, M. Moretti, F. Piccinini, and M. Treccani, J. High Energy Phys. 01 (2007) 013.

[33] F. Paige and S. Protopopescu, in *Supercollider Physics*, edited by D. Sope (World Scientific, Singapore, 1986), p. 320.

[34] C. G. Lester and D. J. Summers, Phys. Lett. B **463**, 99 (1999); H.-C. Cheng and Z. Han, J. High Energy Phys. 12 (2008) 063.

[35] W. S. Cho, K. Choi, Y. G. Kim, and C. B. Park, Phys. Rev. D **79**, 031701 (2009); K. Choi, S. Choi, J. S. Lee, and C. B. Park, Phys. Rev. D **80**, 073010 (2009).

[36] C. Amsler *et al.*, Phys. Lett. B **667**, 1 (2008).

[37] R. Bonciani, S. Catani, M. L. Mangano, and P. Nason, Nucl. Phys. **B529**, 424 (1998).